

## Diffusion bonding of $\text{Ti}_3\text{AlC}_2$ ceramic via a Si interlayer

X. H. Yin · M. S. Li · T. P. Li · Y. C. Zhou

Received: 30 September 2006 / Accepted: 27 December 2006 / Published online: 5 May 2007  
© Springer Science+Business Media, LLC 2007

**Abstract** Based on the structure characteristic of  $\text{Ti}_3\text{AlC}_2$  and the easy formation of  $\text{Ti}_3\text{Al}_{1-x}\text{Si}_x\text{C}_2$  solid solution, a Si interlayer was selected to join  $\text{Ti}_3\text{AlC}_2$  layered ceramic by diffusion bonding method. Joining was performed at 1,300–1,400 °C for 120 min under 5 MPa load in an Ar atmosphere. The phase composition and interface microstructure of the joints were investigated by XRD, SEM and EPMA. The results revealed that  $\text{Ti}_3\text{Al}(\text{Si})\text{C}_2$  solid solution formed at the interface. The mechanism of bonding is attributed to silicon diffusing inward the  $\text{Ti}_3\text{AlC}_2$ . The strength of joints was evaluated by a 3-point bending test. The jointed specimens exhibit a high flexural strength of  $285 \pm 11$  MPa, which is about 80% of that of the  $\text{Ti}_3\text{AlC}_2$ ; and retain this strength up to 1,000 °C. The high mechanical performance of the joints indicates that diffusion bonding via a Si interlayer is effective to bond  $\text{Ti}_3\text{AlC}_2$  ceramic.

### Introduction

The nanolaminate ternary ceramics  $\text{M}_{n+1}\text{AX}_n$  (where M is an early transition metal, A is an A-group element, and X is carbon and/or nitrogen) have attracted extensive attention due to their combination of excellent properties of metals and ceramics [1]. Among these layered ternary compounds,  $\text{Ti}_3\text{AlC}_2$  promoted comprehensive research activities because of its extraordinary mechanical, physical and chemical related properties. The salient properties of this layered ternary ceramic are (other than the merits of high bulk modulus, good damage-tolerance and machinability commonly shared by the ternary carbides of the same family) low density, excellent thermal-shock and oxidation resistance [1–9]. Such unique properties make it possible to use  $\text{Ti}_3\text{AlC}_2$  in structural components for high-temperature applications and as oxidation-resistant coatings on alloy surfaces. However, similar to other ceramics, the synthesis of bulk  $\text{Ti}_3\text{AlC}_2$  with large dimensions is difficult, which limits its wide applications. This limitation can be overcome through joining technology, which allows manufacture of large, complex, multifunctional assemblies through the controlled integrations of smaller, simple, more easily manufacture parts. Joining is a critical enabling technology, essential to the widespread use of ceramics in many applications [10]. Therefore, studies on joining of  $\text{Ti}_3\text{AlC}_2$  ceramic are significant for promoting its applications. However, as far as we are aware, there are no reports on the joining of  $\text{Ti}_3\text{AlC}_2$  ceramic.

Recently, solid solution treatment of MAX phases has attracted increasing attentions. Theoretical and experimental work [11–15] demonstrate that substitutions at the M, A or X sites of MAX phases are totally feasible to form solid solutions. Ganguly et al. [13] fabricated  $\text{Ti}_3\text{Si}_{1-x}\text{Ge}_x\text{C}_2$  solid solutions by substituting Si with Ge. Zhou

---

X. H. Yin · M. S. Li (✉) · T. P. Li · Y. C. Zhou  
High-performance Ceramic Division, Shenyang National  
Laboratory for Materials Science, Institute of Metal Research,  
Chinese Academy of Sciences, 72 Wenhua Road,  
Shenyang 110016, China  
e-mail: mshli@imr.ac.cn

Y. C. Zhou  
e-mail: yczhou@imr.ac.cn

X. H. Yin · T. P. Li  
Graduate School of Chinese Academy of Sciences, Beijing  
100039, China

et al. synthesized  $\text{Ti}_3\text{Si}_{1-x}\text{Al}_x\text{C}_2$  ( $0.01 \leq x \leq 0.15$ ) [16] and  $\text{Ti}_3\text{Al}_{1-x}\text{Si}_x\text{C}_2$  ( $0.05 \leq x \leq 0.25$ ) [17] solid solutions by using in-situ hot pressing/solid liquid reaction process. Their results demonstrated that the high temperature oxidation resistance of  $\text{Ti}_3\text{SiC}_2$  and the mechanical properties of  $\text{Ti}_3\text{AlC}_2$  were dramatically improved due to the solid solution treatment. The formation of  $\text{Ti}_3\text{Si}(\text{Al})\text{C}_2$  solid solution was also proposed when  $\text{Ti}_3\text{SiC}_2$  was aluminized through pack-cementation [18]. It is known that  $\text{Ti}_3\text{AlC}_2$  is isotypic with  $\text{Ti}_3\text{SiC}_2$  and continuous solid solutions can form in the  $\text{Ti}_3\text{SiC}_2$ – $\text{Ti}_3\text{AlC}_2$  family [1]. The addition of Si in  $\text{Ti}_3\text{AlC}_2$  favor the formation of  $\text{Ti}_3\text{Al}(\text{Si})\text{C}_2$  solid solution. Thus, it is possible to bond  $\text{Ti}_3\text{AlC}_2$  using Si as a diffusion interlayer by forming a  $\text{Ti}_3\text{Al}(\text{Si})\text{C}_2$  solid solution.

In this paper, diffusion bonding of layered  $\text{Ti}_3\text{AlC}_2$  ceramic using Si as an interlayer was investigated. The main purpose is to select proper bonding parameters to form  $\text{Ti}_3\text{Al}(\text{Si})\text{C}_2$  joints without deteriorating the excellent properties of  $\text{Ti}_3\text{AlC}_2$  at both room and elevated temperatures.

## Experimental procedures

Bulk  $\text{Ti}_3\text{AlC}_2$  used in this work was synthesized from Ti, Al and graphite powders by in-situ hot pressing/solid-liquid reaction method. Details on the synthesis and characteristics of  $\text{Ti}_3\text{AlC}_2$  were described elsewhere [19]. The measured density of bulk  $\text{Ti}_3\text{AlC}_2$  is  $4.21 \text{ g/cm}^3$  and its relative density is 99%. Specimens with dimensions of  $10 \times 8 \times 2 \text{ mm}^3$  were cut from the as-synthesized bulk ceramic by an electrical-discharge method. The faying face of every specimen was polished to  $1 \mu\text{m}$  diamond paste. Afterwards, the samples were degreased ultrasonically in acetone, cleaned by distilled water and then dried. One Si layer with a thickness of about  $4 \mu\text{m}$  was deposited onto the faying face of some  $\text{Ti}_3\text{AlC}_2$  specimens using a magnetron sputtering system (JGP560C14, China). The magnetron sputtering using a silicon target (purity 99.9%) was conducted at  $300 \text{ }^\circ\text{C}$  in DC mode. The applied power density to the silicon target was kept constant at  $3.2 \text{ W/cm}^2$ . Before deposition, the system was evacuated to a base pressure of  $2 \times 10^{-4} \text{ Pa}$  and the deposition was performed at a total pressure of  $0.6 \text{ Pa}$ . One Si deposited sample and one untreated sample were chosen as a pair of bonding couples. They were placed as face to face to form a sandwich, hence the deposited Si film became an interlayer. In order to find the interface region accurately after the bonding process, one Si deposited sample and one untreated sample were stagger jointed, as shown in Fig. 1. The bonding was conducted in a hot-press furnace under a flowing Ar atmosphere and uniaxial pressure of  $5 \text{ MPa}$ .

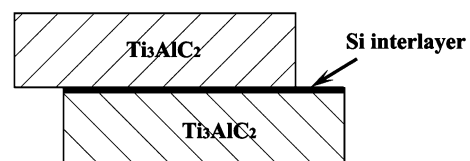


Fig. 1 Schematic illustration of the assembly for bonding

The bonding temperatures range from  $1,300$  to  $1,400 \text{ }^\circ\text{C}$ , while the holding time was set to be  $120 \text{ min}$ . The heating rate was  $15 \text{ }^\circ\text{C/min}$  in all runs, and joints were cooled in furnace after bonding.

In order to determine the bending strength of joints, 3-point bending tests were performed in a universal testing machine at room temperature,  $600$ ,  $800$  and  $1,000 \text{ }^\circ\text{C}$ , respectively. Initially, two  $\text{Ti}_3\text{AlC}_2$  blocks with dimensions of  $20 \times 20 \times 12 \text{ mm}^3$  were bonded. After joining, this bonded specimen was machined into dimensions of  $40 \times 4 \times 3 \text{ mm}^3$  and polished. During bending tests, the crosshead speed was  $0.5 \text{ mm/min}$  and the span was  $30 \text{ mm}$ . The joint was set in the middle of the span. Three samples were tested for each testing condition. When tested at high temperatures, the samples were heated to target temperature and held for  $15 \text{ min}$  to get temperature equilibrium. Because of the excellent oxidation resistance of  $\text{Ti}_3\text{AlC}_2$  at temperatures below  $1,000 \text{ }^\circ\text{C}$  and short annealing time, no attempt was made to avoid the slight oxidation of the samples.

The joint interface and fracture surface were investigated by a scanning electron microscope (SEM, LEO, Germany) equipped with energy-dispersive X-ray spectroscopy (EDS) system. After bonding, the sample was sliced in the direction perpendicular to the staggered joint and polished. SEM investigation was carried out along the staggered line. The distributions of elements were determined by electron probe microanalysis (EPMA1610, Shimadzu, Japan). The accelerating voltage was  $15 \text{ kV}$  and estimated volume of interaction was about  $3 \mu\text{m}^3$ . For all cases, the standard deviation of the measured intensity for a single measurement did not exceed 2% relative. Quantitative analysis was performed using a conventional ZAF correction procedure. The accuracy of the indicated procedure was checked on a bulk uniform standard of TiC.

The phase compositions of the interface were analyzed by X-ray diffraction (XRD). The XRD data were collected by a step-scanning diffractometer with  $\text{CuK}_\alpha$  radiation (Rigaku D/max-2400, Japan). To identify the change in lattice parameters of  $\text{Ti}_3\text{AlC}_2$  after bonding, the complete profile of the powder diffraction pattern was refined by the Rietveld method employing the DBWS code in the Cerius<sup>2</sup> computational program for materials research (Molecular Simulation, Inc., USA). The intensity is represented by:

$$I_{\text{Rietveld}}(2\theta) = b(2\theta) + s \sum_K L_K |F_K|^2 \phi(2\theta_i - 2\theta_K) P_K A_K, \tag{1}$$

where  $b(2\theta)$  is the background intensity,  $s$  is a scale factor,  $L_K$  contains the Lorentz, polarization and multiplicity factors,  $\phi$  is the profile function,  $P_K$  is the preferred orientation function,  $A_K$  is the absorption factor and  $F_K$  is the structure factor. The index  $K$  represents Miller indices for the Bragg reflections. To measure peak angles accurately, each tested peak was scanned with a slow scanning step of  $0.02^\circ$  and a scan rate of  $0.5^\circ/\text{min}$ .

**Results and discussion**

All of the  $\text{Ti}_3\text{AlC}_2$  couples could be joined apparently. Figure 2a, b present the cross-sectional views of typical microstructures of  $\text{Ti}_3\text{AlC}_2/\text{Si}/\text{Ti}_3\text{AlC}_2$  couples bonded at  $1,300^\circ\text{C}$  (Fig. 2a) and  $1,400^\circ\text{C}$  (Fig. 2b) for 120 min under 5 MPa, respectively. Clearly, when bonded at  $1,300^\circ\text{C}$ , one layer of Si remained at the interface. This indicates that bonding was not complete. However, when bonded at  $1,400^\circ\text{C}$ , the Si interlayer disappeared completely. Reaction zone, pores or original bond line were not observed at the interface. The residual silicon layer may

deteriorate the mechanical properties of the joints, especially at high temperatures, so thereafter all joints were made at  $1,400^\circ\text{C}$ .

To identify the depth profile of silicon in the  $\text{Ti}_3\text{AlC}_2$  substrate, EPMA analysis was conducted. Figure 3 shows the distributions of elements obtained by a line scan analysis of EPMA across the joint of  $\text{Ti}_3\text{AlC}_2$  ceramic after bonding at  $1,400^\circ\text{C}$  for 120 min under 5 MPa. It can be seen that in the whole analysis region, the contents of Ti, Al and C are almost constant, and their corresponding atomic ratio is about 3:1:2, which is similar to that of the  $\text{Ti}_3\text{AlC}_2$  substrate. It is also noted that Si diffused inward so quickly that it distributes across the whole thickness of the sample. Moreover, the distribution of Si is homogenous and its mean concentration is about 0.38 at.%. According to the result of EPMA, the solid solution of Si in  $\text{Ti}_3\text{AlC}_2$  can be written as  $\text{Ti}_3\text{Al}_{0.98}\text{Si}_{0.02}\text{C}_2$ .

To identify the phase composition of the interface, XRD analysis was conducted on the powders prepared by drilling from the area of the joint interface. Figure 4 shows the X-ray diffraction pattern of powder from the joint bonded at  $1,400^\circ\text{C}$  for 120 min under 5 MPa. For comparison, XRD pattern of powder from  $\text{Ti}_3\text{AlC}_2$  is also presented. As shown in Fig. 4, the phase of the joint can be indexed using the structure of  $\text{Ti}_3\text{AlC}_2$ . No new reaction phases can be detected within the resolution of the X-ray diffractometer. However, by careful analysis of the XRD patterns in Fig. 4, it can be seen that the reflection peaks shift to large angles after bonding process, which suggests that Si diffused into  $\text{Ti}_3\text{AlC}_2$  and the formation of  $\text{Ti}_3\text{Al}(\text{Si})\text{C}_2$  solid solution. To quantitatively determine the change of lattice parameters, Rietveld refinement of the diffraction patterns was

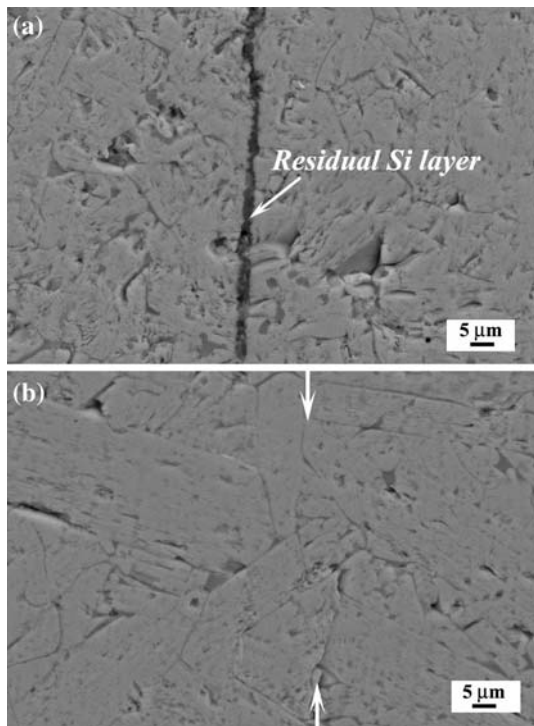


**Fig. 2** Backscattered SEM images of the interfacial structure of the  $\text{Ti}_3\text{AlC}_2/\text{Si}/\text{Ti}_3\text{AlC}_2$  couples treated at (a)  $1,300^\circ\text{C}$  and (b)  $1,400^\circ\text{C}$  for 120 min under 5 MPa. Arrows denote the interface

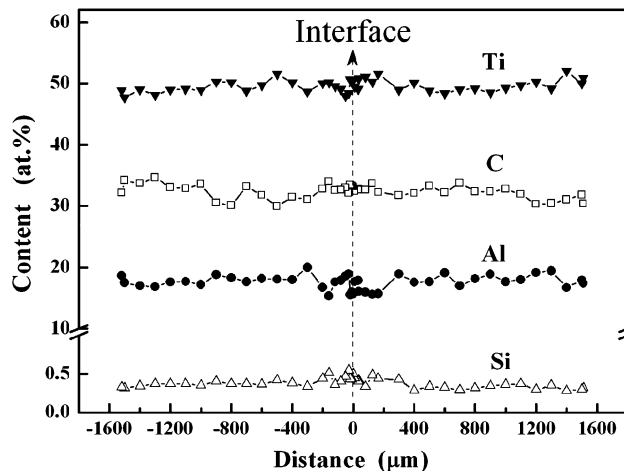


**Fig. 3** Depth profiles of constituent elements obtained by EPMA on the  $\text{Ti}_3\text{AlC}_2/\text{Si}/\text{Ti}_3\text{AlC}_2$  joint bonded at  $1,400^\circ\text{C}$  for 120 min under 5 MPa. The contents of Ti, Al and C are almost constant, and their corresponding atomic ratio is about 3:1:2. Si diffused inward so quickly that it distributes across the whole thickness of the sample. Arrow denotes the interface

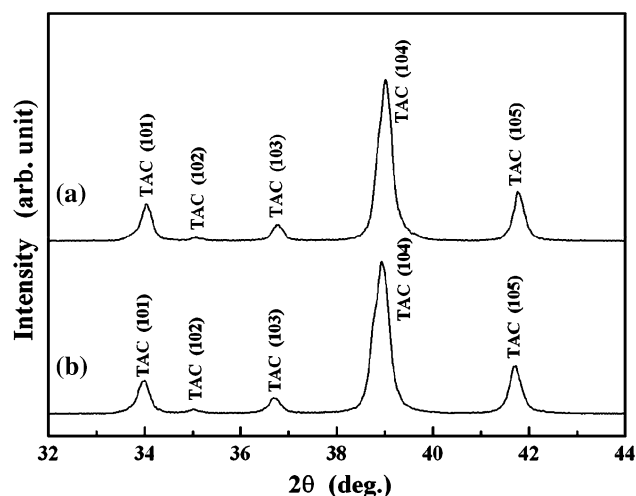


**Fig. 4** X-ray diffraction patterns of (a) the  $\text{Ti}_3\text{AlC}_2/\text{Si}/\text{Ti}_3\text{AlC}_2$  joint bonded at 1,400 °C for 120 min under 5 MPa and (b)  $\text{Ti}_3\text{AlC}_2$

performed using  $\text{Ti}_3\text{AlC}_2$  as the structure model. In all refinement, the reliability factors (R-P and R-WP values are 6.57 and 9.49%, respectively) are less than 10%. The calculated lattice parameters  $a$  and  $c$  of the  $\text{Ti}_3\text{Al}(\text{Si})\text{C}_2$  solid solution and  $\text{Ti}_3\text{AlC}_2$  are listed in Table 1. The lattice parameters of standard  $\text{Ti}_3\text{AlC}_2$  sample are  $a = 0.3074$  nm,  $c = 1.8556$  nm, these values agree well with those reported in previous works [17, 20]. The lattice parameters of  $\text{Ti}_3\text{Al}(\text{Si})\text{C}_2$  are  $a = 0.3072$  nm,  $c = 1.8526$  nm, which are smaller than those of  $\text{Ti}_3\text{AlC}_2$ . This trend is consistent with the previous result [17], and provides an compelling evidence of the formation of  $\text{Ti}_3\text{Al}(\text{Si})\text{C}_2$  solid solution at the interface. Furthermore, according to the equation that describes the  $c$  axis change with Si content in the  $\text{Ti}_3\text{Al}(\text{Si})\text{C}_2$  solid solution [17]:

$$c(x) = 1.8541 - (8.5674 \times 10^{-2})x, \quad (2)$$

where  $x$  is the Si content.  $\text{Ti}_3\text{Si}(\text{Al})\text{C}_2$  solid solution can be described as  $\text{Ti}_3\text{Si}_{0.98}\text{Al}_{0.02}\text{C}_2$ . This is in good agreement with the EPMA analysis mentioned above.

Based on the results of SEM, EPMA and XRD analysis, it can be concluded that silicon diffused into  $\text{Ti}_3\text{AlC}_2$  to

**Table 1** Lattice parameters (in nm) and  $c/a$  ratio of  $\text{Ti}_3\text{AlC}_2$ ,  $\text{Ti}_3\text{Al}(\text{Si})\text{C}_2$ ,  $\text{Ti}_3\text{Al}_{0.95}\text{Si}_{0.05}\text{C}_2$ , and  $\text{Ti}_3\text{Al}_{0.9}\text{Si}_{0.1}\text{C}_2$

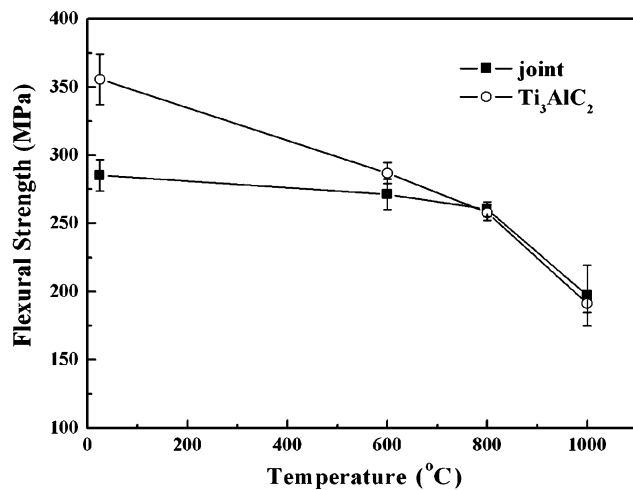
	$a$	$c$	$c/a$	Remarks
$\text{Ti}_3\text{AlC}_2$	0.3074	1.8556	6.037	This work
	0.3073	1.8539	6.034	Ref. [17]
	0.3075	1.858	6.042	Ref. [20]
$\text{Ti}_3\text{Al}(\text{Si})\text{C}_2$ (Joint)	0.3072	1.8526	6.030	This work
$\text{Ti}_3\text{Al}_{0.95}\text{Si}_{0.05}\text{C}_2$	0.3073	1.8496	6.019	Ref. [17]
$\text{Ti}_3\text{Al}_{0.9}\text{Si}_{0.1}\text{C}_2$	0.3073	1.8456	6.004	Ref. [17]

form a  $\text{Ti}_3\text{Al}(\text{Si})\text{C}_2$  solid solution at the interface during the bonding process. In fact, continuous solid solutions exist in  $\text{Ti}_3\text{SiC}_2$ – $\text{Ti}_3\text{AlC}_2$  system [1], and Zhou et al. synthesized  $\text{Ti}_3\text{Al}_{1-x}\text{Si}_x\text{C}_2$  ( $0.05 \leq x \leq 0.25$ ) [17] solid solutions. It is apt for Si to diffuse inward  $\text{Ti}_3\text{AlC}_2$ , which is related to the crystal structure characteristic of  $\text{Ti}_3\text{AlC}_2$ .  $\text{Ti}_3\text{AlC}_2$  crystallizes in a space group of  $P6_3/mmc$  symmetry and its crystal structure can be regarded as two edge-shared  $\text{Ti}_6\text{C}$  octahedral being weakly bonded with the interleaved planar closed-packed Al atomic layer [20]. The weak bonding between Ti–C–Ti–C–Ti covalent bond chain and the adjacent Al atoms is beneficial to the intercalation of Si into  $\text{Ti}_3\text{AlC}_2$ . Moreover, the diameter of Si atom is smaller than that of Al atom, therefore Si atom can diffuse inward  $\text{Ti}_3\text{AlC}_2$  easily. Bulk  $\text{Ti}_3\text{AlC}_2$  has a layered microstructure, these interlamination supplies a great number of rapid diffusion paths for Si.

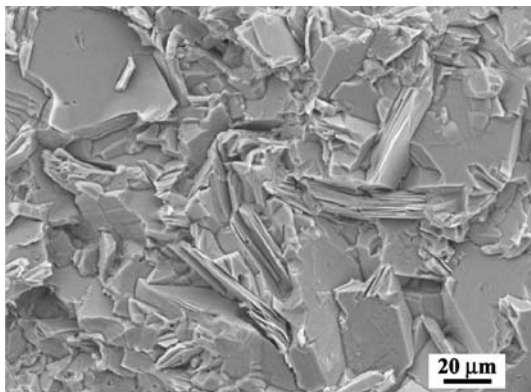
Interestingly, Si diffused inward so quickly that it distributed across the whole thickness of the  $\text{Ti}_3\text{AlC}_2$  sample. Li et al. [18] have observed the similar phenomenon when  $\text{Ti}_3\text{SiC}_2$  was aluminized through pack-cementation. They found that a part of Al diffused into the whole  $\text{Ti}_3\text{SiC}_2$  bulk sample to form  $\text{Ti}_3\text{Si}(\text{Al})\text{C}_2$  solid solution. Assuming that Si diffuses inward  $\text{Ti}_3\text{AlC}_2$  completely and distributes homogeneously, the content of Si in the  $\text{Ti}_3\text{Al}(\text{Si})\text{C}_2$  solid solution should be 0.76 at.% based on the theoretical calculation. However, the mean concentration of Si is 0.38 at.%, which is lower than the theoretical value (0.76 at.%). Apart from the measurement error, several explanations can be given for this difference. One is that Si may segregate at the grain boundaries of  $\text{Ti}_3\text{AlC}_2$ . Another is due to the consumption of Si as  $\text{SiO}$  gas formed by the reaction of Si with oxygen at low oxygen partial pressure [21].

Figure 5 shows the measured flexural strength of the joint bonded at 1,400 °C for 120 min as a function of testing temperature. For comparison, the flexural strength of  $\text{Ti}_3\text{AlC}_2$  tested under the same condition is also presented in Fig. 5. The flexural strength of the joint at room temperature is  $285 \pm 11$  MPa, which is about 80% of that of the  $\text{Ti}_3\text{AlC}_2$  substrate. With increasing temperature, the flexural strength of the joint decrease at a rate lower than that of  $\text{Ti}_3\text{AlC}_2$ . When the temperature is higher than 800 °C, both the joint and  $\text{Ti}_3\text{AlC}_2$  have roughly the same flexural strength. At 1,000 °C, the strength of joint remains  $197 \pm 22$  MPa. These results indicate that a joint with good mechanical strength can be achieved through diffusion bonding and may meet the requirements of high temperature applications.

The fractured specimens were examined by scanning electron microscope. It was found that samples failed along the joint, and no residual Si was detected on the fracture surface. Figure 6 shows the morphology of the fractured



**Fig. 5** Flexural strength of the joint and Ti<sub>3</sub>AlC<sub>2</sub> substrate as a function of testing temperatures



**Fig. 6** Scanning electron micrograph of the fracture surface of the joint bonded at 1,400 °C for 120 min under 5 MPa. No residual Si was detected on the fracture surface

surface of the joint treated at 1,400 °C for 120 min under 5 MPa. The characteristic of the laminated Ti<sub>3</sub>AlC<sub>2</sub> grain can be obviously seen from Fig. 6. These observations confirm that Si diffuses into the Ti<sub>3</sub>AlC<sub>2</sub> substrate.

Generally, if no defects exist at the interface, the strength of a joint is mainly related to its composition, interfacial microstructure, and the residual stress resulting from mismatch of thermal expansion coefficient (TEC) during cooling from bonding temperature to ambient temperature. In the present work, due to the formation of Ti<sub>3</sub>Al(Si)C<sub>2</sub> solid solution, the joint has a similar microstructure with the parent material. Zhou et al. [17] have proved that the mechanical properties of Ti<sub>3</sub>Al<sub>x</sub>Si<sub>1-x</sub>C<sub>2</sub> solid solution ( $x \leq 0.1$ ) were slightly higher than that of Ti<sub>3</sub>AlC<sub>2</sub>. Consequently, the formation of Ti<sub>3</sub>Al(Si)C<sub>2</sub> solid solution should be beneficial to increasing the joint strength. Moreover, Si solid solution could not affect the TEC value of Ti<sub>3</sub>AlC<sub>2</sub> obviously, both Ti<sub>3</sub>Al(Si)C<sub>2</sub> solid

solution and Ti<sub>3</sub>AlC<sub>2</sub> have a close value of TEC [22]. Consequently, the residual stress in the joint should be neglected.

## Conclusion

Strong joints of Ti<sub>3</sub>AlC<sub>2</sub> ceramic can be achieved through diffusion bonding via a Si interlayer. SEM, EPMA and XRD analyses revealed that Ti<sub>3</sub>Al(Si)C<sub>2</sub> solid solution forms at the interface during bonding process. The mechanism of bonding is attributed to the inward diffusion of Si. The formation of Ti<sub>3</sub>Al(Si)C<sub>2</sub> solid solution causes the joint to possess a high strength, owing to similar mechanical properties and TEC value of Ti<sub>3</sub>Al(Si)C<sub>2</sub> solid solution to that of Ti<sub>3</sub>AlC<sub>2</sub> substrate. The room temperature flexural strength of the joint bonded at 1,400 °C for 120 min under 5 MPa is 285 ± 11 MPa, which is about 80% of that of the Ti<sub>3</sub>AlC<sub>2</sub> substrate. At 1,000 °C, the flexural strength of the joint is still as high as 197 ± 22 MPa, roughly in the same level of Ti<sub>3</sub>AlC<sub>2</sub>.

**Acknowledgements** This work was supported by the National Science Foundation of China under Grant Nos. 50371095, 50232040, 50302011, 90403027; and cooperation project of Chinese Academy of Sciences and French Atomic Energy Commission.

## References

1. Barsoum MW (2000) Prog Solid Chem 28:201
2. Wang XH, Zhou YC (2002) Acta Mater 50:3141
3. Tzenov NV, Barsoum MW (2000) J Am Ceram Soc 83:825
4. Lopacinski M, Puszynski J, Lis J (2001) J Am Ceram Soc 84:3051
5. Zhou YC, Wang XH (2001) J Mater Chem 11:2335
6. Bao YW, Chen JX, Wang XH, Zhou YC (2004) J Eur Ceram Soc 24:855
7. Bao YW, Wang XH, Zhang HB, Zhou YC (2005) J Eur Ceram Soc 25:3367
8. Wang XH, Zhou YC (2003) Corros Sci 45:891
9. Wang XH, Zhou YC (2003) Chem Mater 15:3716
10. Loehman RE, Tomsia AP (1988) Am Ceram Soc Bull 67:375
11. Sun ZM, Ahuja R, Scheider JM (2003) Phys Rev B 68:224112
12. Meng FL, Zhou YC, Wang JY (2005) Scripta Mater 53:1369
13. Ganguly A, Zhen T, Barsoum MW (2004) J Alloys Compd 376:287
14. Barsoum MW, Ali M, El-Raghy T (2000) Metall Mater Trans 31A:1857
15. Wang JY, Zhou YC (2003) J Phys: Condens Matter 15:5959
16. Zhou YC, Zhang HB, Liu MY, Wang JY, Bao YW (2004) Mater Res Innov 8:97
17. Zhou YC, Chen JC, Wang JY (2006) Acta Mater 54:1317
18. Li M, Liu G, Zhang Y, Zhou Y (2003) Oxid Metal 60:179
19. Wang XH, Zhou YC (2002) J Mater Chem 12:455
20. Pietzka MA, Schuster JC (1994) J Phase Equilib 15:392
21. Gulbransen EA, Andrew KF, Brassar FA (1966) J Electrochem Soc 113:834
22. Chen JX (2005) Methods of strengthening layered machinable ternary ceramic Ti<sub>3</sub>AlC<sub>2</sub>. PhD thesis, Inst. Met. Res., CAS, p 102